ISSN No:-2456-2165 https://doi.org/10.38124/ijisrt/25mar1591

Ampacity of Multi-Circuit Overhead Power Lines with Different Routes

Mehmet Yılmaz[1]

[1]B. Sc; Ph.D;
Faculty of Arts and Sciences, Department of Physics,
Yıldız Technical University Istanbul, Türkiye

Publication Date: 2025/04/09

Abstract: The continuous current carrying capacity is related to continuous loading. Bare conductors in overhead power lines (OHL) are under atmospheric conditions. In this respect, the air temperature, wind speed, and solar potential of the region can play a role in increasing or decreasing the current carrying capacity. Due to the heat balance, similar to Kirchhoff's current law, the heat gained and lost by the conductor are equal. If a multi-circuit power line is on the same tower, the current carrying capacities are equal since the phases of each circuit are exposed to the same meteorological parameters. If the circuits of a multi-circuit power line are on separate towers and pass through different routes, in this case, each circuit will be affected by different meteorological parameters and the current carrying capacities will not be equal. In this article, the degree of asymmetry in the steady state current carrying capacity of each circuit in multi-circuit power lines passing through different routes is examined. Depending on the length and geographical features of the route, meteorological parameters in each line segment were taken into account instead of the average meteorological parameters along the line.

Keywords: *Ampacity, IEC Standard 738, IEEE 61597, Multi-Conductor Line, Heat Balance.*

How to Cite: Mehmet Yılmaz. (2025). Ampacity of Multi-Circuit Overhead Power Lines with Different Routes. *International Journal of Innovative Science and Research Technology*, 10(3), 2448-2457. https://doi.org/10.38124/ijisrt/25mar1591.

I. INTRODUCTION

When current is drawn from a conductor, “Joule heat” is generated due to I^2R losses, and the conductor will also gain “solar heat” due to the sun. These two heats gained will be released to the atmosphere through “radiation” and “convection”. There is also the “corona heat” and “magnetic heat” that the conductor will gain, as well as the heat lost through “evaporation”; however, since these heats are very small compared to the joule, solar, radiation and convection heats, they are usually neglected. The “heat balance equation” is written for the joule, solar, radiation and convection heats, and if the current is left on the left of the equation at the end of the intermediate processes, the continuous current carrying capacity of the conductor I (A) is found.

Different formulas can be used under different assumptions in the calculation of the current carrying capacity of conductors used in overhead lines. The standards and technical documents used in the world for the calculation of current carrying capacity are as follows:

- IEEE Standard 738 [1]
- IEC 61597 [2]
- CIGRÈ Brochures [3, 4]
- ESAA Standard (Australia) [5]

In all of the above standards/technical documents, the calculation of current carrying capacity is based on the equivalence of the heat gained by the conductor and the heat lost. The difference in the standard used does not cause significant differences in the calculated current carrying capacity [6-9].

Overhead power lines are naturally under the influence of atmospheric parameters throughout the year. Atmospheric parameters greatly affect the current carrying capacity (ampacity) of the power transmission line [10-12].

For example, air temperature plays a role in reducing the current carrying capacity of the power transmission line [13-16].

Because air temperature is heat gain for the conductor. In the summer months, especially during the daytime, since the conductor gains solar energy and the ambient temperature reaches the highest value, the current carrying capacity of the conductor decreases. However, since the wind effect has a cooling feature on the conductor, the current carrying capacity of the overhead line conductor increases as the wind speed increases [17, 18]. Since a part of the heat in the conductor is also given to the atmosphere by radiation, radiation also positively affects the current carrying capacity of the conductor.

ISSN No:-2456-2165 https://doi.org/10.38124/ijisrt/25mar1591

Not only meteorological parameters affect the current carrying capacity of the conductor, but also the diameter and emission coefficient of the conductor. The emission coefficient of the conductor gets higher as the conductor ages. According to the observations made on ACSR conductors, the emission coefficient is low in new conductors, while it is high in old (used for many years) conductors. In summary, there is a close relationship between the emission coefficient of the ACSR conductor and its operating life [19].

Three current carrying capacities are defined for overhead power lines from a thermal perspective [20]:

- Steady state line ampacity
- Dynamic line ampacity (for t<30 minutes)
- Transient line ampacity (for t<a few seconds)

In addition to analytical methods, numerical methods are also used in the calculation of the continuous current carrying capacity of overhead power lines [21-23].

Nowadays, AC power transmission lines are made not as single-circuit but as double-circuit or multi-circuit, depending on the transmission distance, transmitted power and operating voltage. While a single-circuit (n=1) AC power transmission line contains 3 phases (a b c), for example, a double-circuit transmission line (n=2) contains a b c phases and a′ b′ c′ phases. If n>2, it is understood that the power transmission line is multi-circuit. The "circuit number" of power transmission lines is determined depending on the power to be transmitted (MW), transmission distance (km) and annual demand increase rate (%) [24, 25].

➢ *Multi-Circuit Power Lines Provide the Following Advantages:*

- As the transmission distance increases, the resistance of the transmission lines increases, thus increasing joule losses. When the power line is made as multi-circuit, joule losses decrease.
- The voltage drop of a multi-circuit power line is equal to 1/n times the voltage drop of a single-circuit power line.
- The unit construction cost (ESD/km, EUR/km) of multi-circuit power lines is more economical; savings in assembly costs and expropriation costs play a role in this.
- More secure uninterrupted operation is provided with multi-circuit power transmission lines, reliability is higher in these lines.
- Multi-circuit power transmission lines perform better in terms of stability than single-circuit power transmission lines.
- It is possible to transmit very large powers to very long distances by increasing the number of bundles and operating voltage in multi-circuit power transmission lines.
- Today, multi-circuit pole designs can be easily realized even for large spans such as river crossings.

In this article, the current carrying capacity of multi-circuit power transmission lines that are not located on the same pole and have different route characteristics is examined.

II. AMPACITY OF A BARE CONDUCTOR

The thermal current carrying capacity of an ACSR (Aluminum Conductor Steel Reinforced) conductor is found by equalizing the heat gained and lost by the conductor:

$$\text{Heat gain} = \text{Heat loss} \quad (1)$$

$$P_J + P_S = P_C + P_R \quad (2)$$

Where P_J joule heating, P_S solar heating, P_C convection loss and P_R radiation loss. $P_J = R_{AC}\times I^2$.

If $P_J = R_{AC}\times I^2$ is written above, the thermal current that will provide the heat balance is calculated:

$$I_{th} = \sqrt{\frac{P_C+P_R-P_S}{R_{AC}}} \quad (3)$$

Where P_C, P_R, P_S and R_{AC} are calculated as

$$P_R = e\times 5.7\times 10^{-8}\times\pi\times d\,(T_C^4 - T_A^4) \quad (4)$$

$$P_C = 8.55\,(T_C - T_A)\times(v\times d)^{0.448} \quad (5)$$

$$P_S = a\times S\times d \quad (6)$$

$$R_{AC} = k_s\times R_{DC} \quad (7)$$

Here:

e: Emission coefficient of the conductor (For 500 W/m2 solar radiation, the ratio of "current carrying capacity of the old ACSR conductor/current carrying capacity of the new ACSR conductor" is ≈ 1.1, while for 1000 W/m2 this ratio is ≈ 1.05 [19])
a: Solar radiation coefficient
S: Solar radiation intensity (W/m2)
T_C: Temperature of the conductor $T_C = 273 + T_J + T_{max}$
T_A: Temperature of the environment $T_A = 273 + T_{max}$
T_J: Assumed temperature gained by the conductor due to Joule losses (°C)
T_{max}: Maximum ambient temperature of the region (°C)
d: Diameter of the conductor (m)
v: Wind speed (m/s)
5.7×10^{-8}: Stefan-Boltzmann constant

R_{DC}: Direct current resistance of the conductor at $T_J + T_{max}$ temperature (Ω/m)
R_{AC}: : Alternating current resistance of the conductor at temperature $T_J + T_{max}$ (Ω/m)
k_s: skin effect factor

The AC resistance R1 of the ACSR conductor at temperature T1 (e.g. 20 °C) and the AC resistance R2 at temperature T2 have the following relationship:

ISSN No:-2456-2165 https://doi.org/10.38124/ijisrt/25mar1591

$$R_2 = R_1 \times \left(\frac{228.1+T_2}{228.1+T_1}\right) \quad (8)$$

There are various empirical relations for the calculation of skin effect factor. For example, one of these relations is the following [26]:

$$k_s = a_0 + a_1 x + a_2 x^2 + a_3 x^3 + a_4 x^4 \quad (9)$$

$$x = \sqrt{\frac{f\,(Hz)}{R_{DC}\,(\frac{\Omega}{km})}} \quad (10)$$

The "a" coefficients are obtained depending on the ratio of the number of aluminum cores/number of steel cores in the ACSR conductor. For example, for ACSR 54/7 and 54/19, the "a" coefficients take the following values: a_0 = 0.99979, a_1 = 6.2538×10^{-5}, a_2 = −6.4912×10^{-6}, a_3 = 2.8143×10^{-7} and a_4 = 1.4862×10^{-8}. For ACSR 30/7, it takes the values a_0 = 0.99992, a_1 = 2.6909×10^{-5}, a_2 = −2.9508×10^{-6}, a_3 = 1.3297×10^{-7} and a_4 = 1.2010×10^{-8} [26].

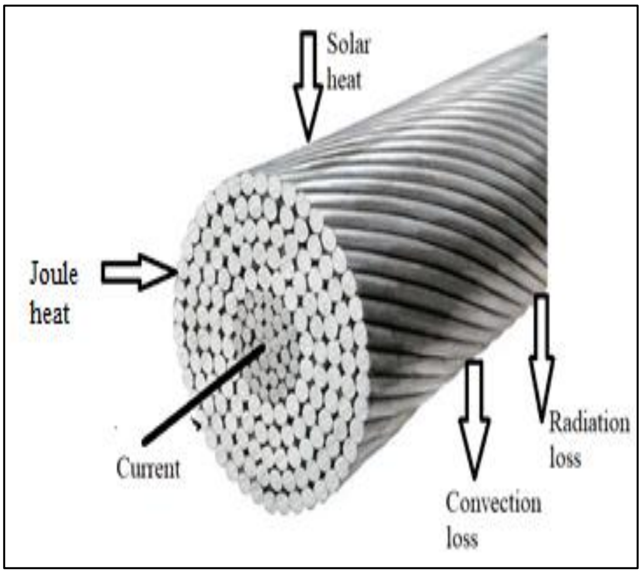

Fig 1: Heat Gains and Heat Losses of an ACSR Conductor

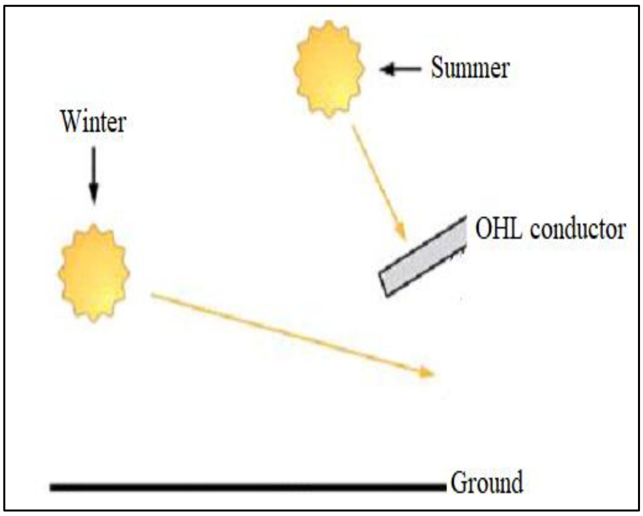

Fig 2: Effect of Solar Radiation on ACSR Conductor in Summer and Winter Months

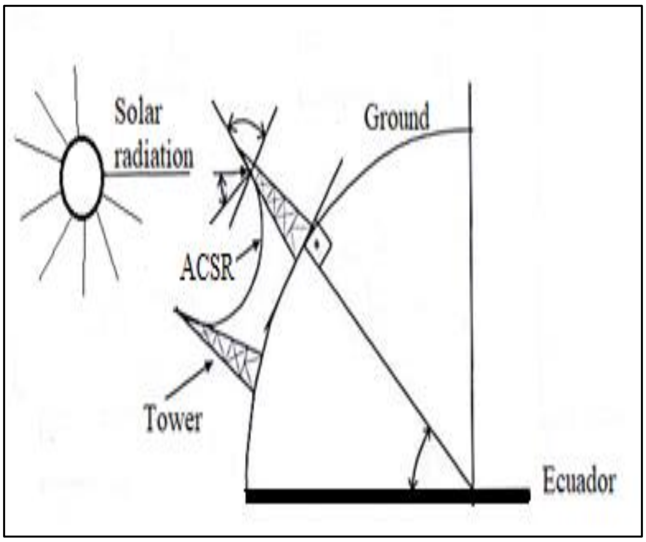

Fig 3: Effect of Solar Radiation on ACSR Conductor Depending on its Location on the Earth

The sun map and wind map taken into consideration in the thermal dimensioning of power systems in Turkey are shown in Figure 4 and Figure 5.

In the ice load map for the design of power transmission lines in Turkey, five regions (I, II, III, IV, V) are defined; the maximum air temperature in these regions is accepted as 50 °C in Region I, 45 °C in Region II and 40 °C in other regions. When the altitude of a region above sea level exceeds a certain value, the values of the upper region are taken as basis.

ISSN No:-2456-2165 https://doi.org/10.38124/ijisrt/25mar1591

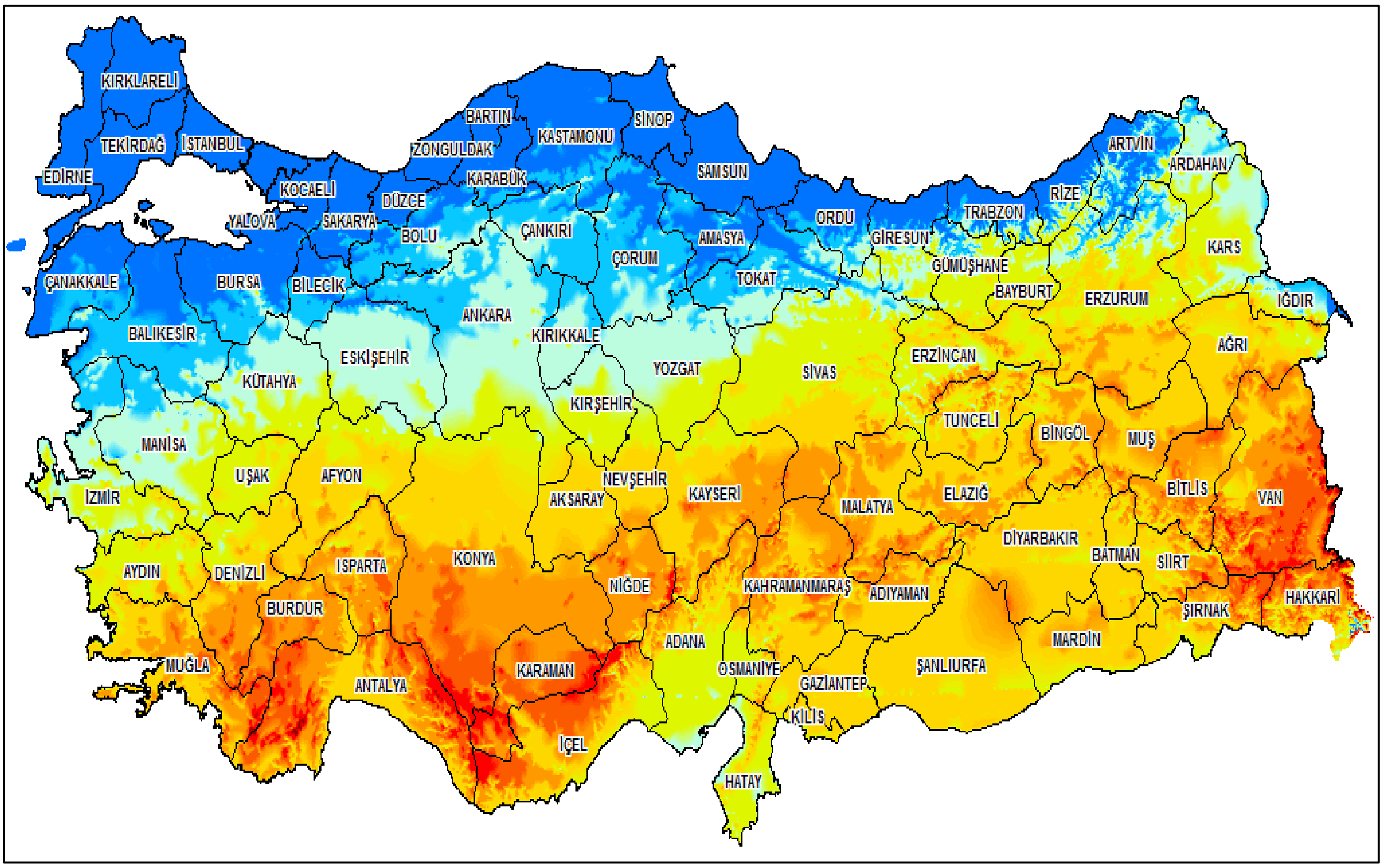

Fig 4: Türkiye Sun Map (Light Colored Areas Receive Intense Sunlight)
[Source: Turkish State Meteorological Service]

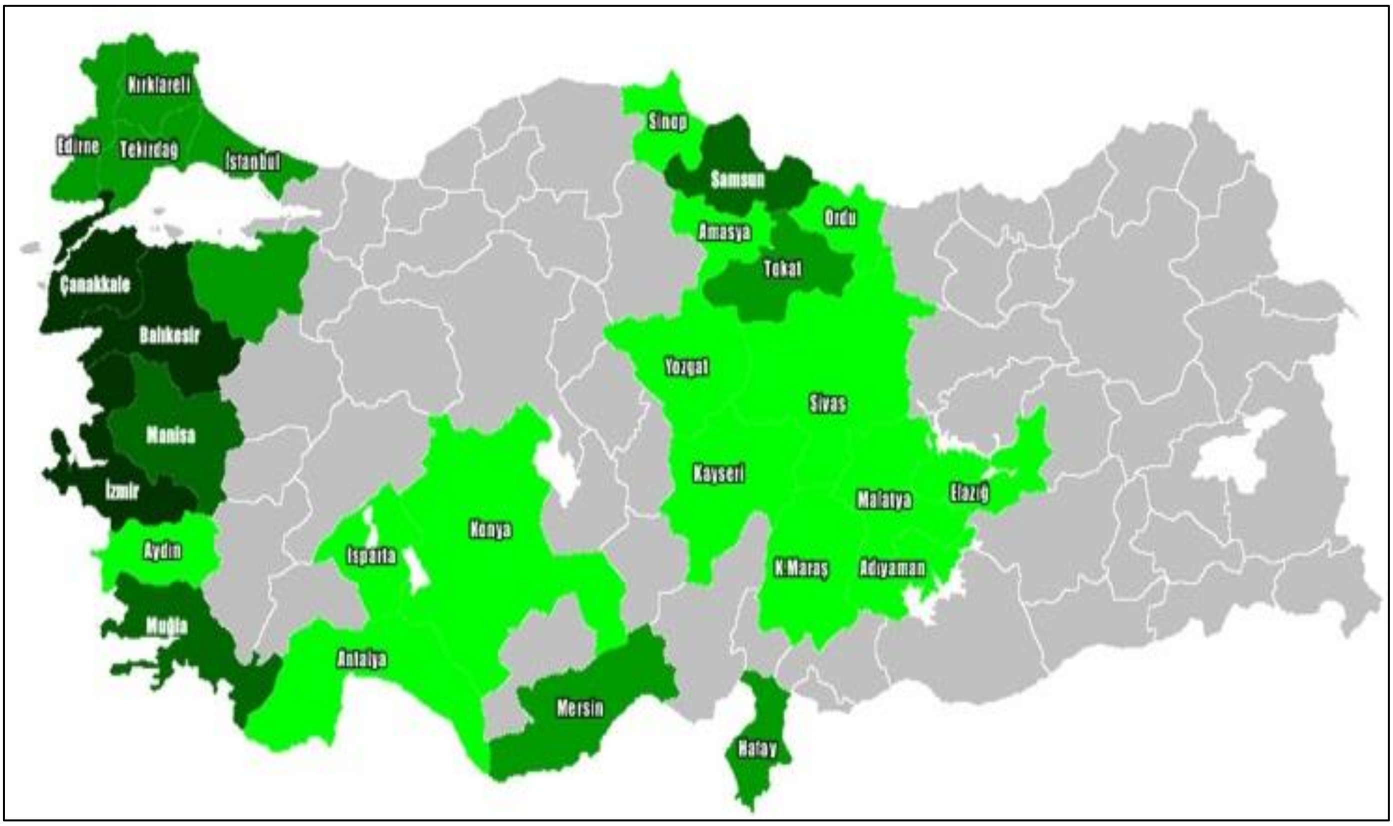

Fig 5: Türkiye Wind Map (Dark Areas Receive Intense Winds)
[Source: Turkish State Meteorological Service]

ISSN No:-2456-2165 https://doi.org/10.38124/ijisrt/25mar1591

Seasonal thermal capacities of 400 kV and 154 kV power transmission lines in Turkey are given in Table 1 and Table 2.

Table :1 Types and Capacities of Conductors used in 400 kV Transmission Lines in Turkey

Conductor type	**Cross-sectional area (mm^2)**	**Ampacity (A)[3]**	**Summer capacity (MVA)[1]**	**Spring capacity (MVA)[2]**	**Thermal capacity (MVA)[3]**
2B[4], Rail	2×517	2×755	832	1360	995
2B[4], Cardinal	2×547	2×765	845	1360	1005
3B4, Cardinal	3×547	3×765	1268	2070	1510
3B[4], Pheasant	3×726	3×925	1524	2480	1825

[Source: Turkish Electrical Grid Regulation]
[1]Conductor Temperature: 80 ºC, Air Temperature:40 ºC, Wind Speed: 0.1 m/s
[2]Conductor Temperature:80 ºC, Air Temperature:25 ºC, Wind Speed: 0.5 m/s
[3]Conductor Temperature:80 ºC, Air Temperature: 40 ºC, Wind Speed: 0.25 m/s
[4]Bundle conductor (2B: twin bundle, 3B: triple bundle)

Table 2: Types and Capacities of Conductors used in 154 kV Transmission Lines in Turkey

Type	**Cross-sectional area (mm^2)**	**Ampacity (A)[3]**	**Summer capacity (MVA)[1]**	**Spring capacity (MVA)[2]**	**Thermal capacity (MVA)[3]**
Hawk	281	496	110	180	132
Drake	468.4	683	153	250	182
Cardinal	547	765	171	280	204
2B Cardinal	2×547	2×765	342	560	408
Pheasant	726	925	206	336	247

[Source: Turkish Electrical Grid Regulation]
[1]Conductor Temperature: 80 ºC, Air Temperature: 40 ºC, Wind Speed: 0.1 m/s
[2]Conductor Temperature: 80 ºC, Air Temperature: 25 ºC, Wind Speed: 0.5 m/s
[3]Conductor Temperature: 80 ºC, Air Temperature: 40 ºC, Wind Speed: 0.25 m/s

The calculation of current carrying capacity in multi-circuit power transmission lines is the same as the calculation for single-circuit transmission lines if all circuits are on the same pole (Fig. 6), because all conductors on the same pole are under the influence of the same meteorological parameters.

Fig 6: Tek Devreli Ve Aynı Direk Üzerindeki İki Devreli Ve Dört Devreli İletim Hatları

If the power drawn from a multi-circuit power transmission line is P (MW), the operating voltage is U (kV), the power factor of the load is cos ϕ, the number of circuits is n_c and the number of bundles is n_b, the current passing through an ACSR conductor is calculated as follows:

$$I_{ACSR} = \frac{P/(n_c \times n_b)}{\sqrt{3} \times U \times \cos\phi} \quad \ldots(\text{kA}) \qquad (11)$$

For the thermally appropriate design of the ACSR conductor, the following conditions must be met:

$$I_{ACSR} \leq I_{th} \qquad (12)$$

Where

I_{th} is the maximum current carrying capacity of the ACSR conductor as specified in the catalogue.

ISSN No:-2456-2165 https://doi.org/10.38124/ijisrt/25mar1591

III. AMPACITY OF MULTI-CIRCUIT POWER TRANSMISSION LINES WITH DIFFERENT ROUTES

➢ *The Different Routes of Multi-Circuit Power Transmission Lines may be due to the Following Reasons:*

- Route difficulties (proximity to active faults, swamps, densely populated areas, etc.)
- Addition of a new circuit to the existing transmission line as a result of increasing power transmission demand
- Dismantling and relocating some circuits to different routes as a result of changes in the settlement plans in the region over time.

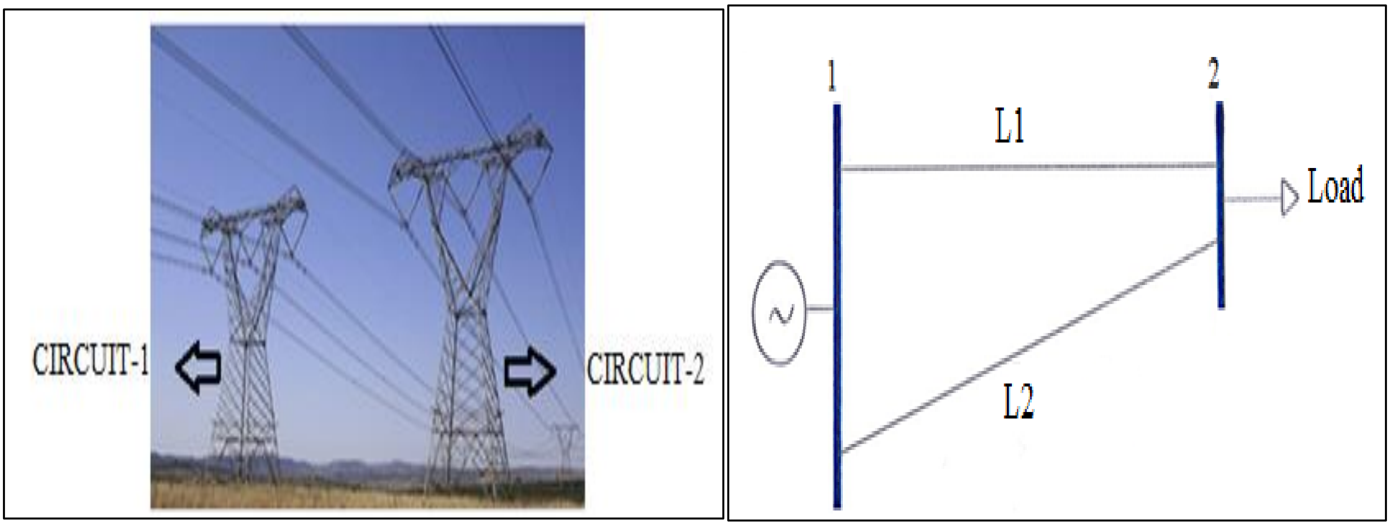

Fig 7: Double circuit transmission line and single line diagram with different routes and lengths

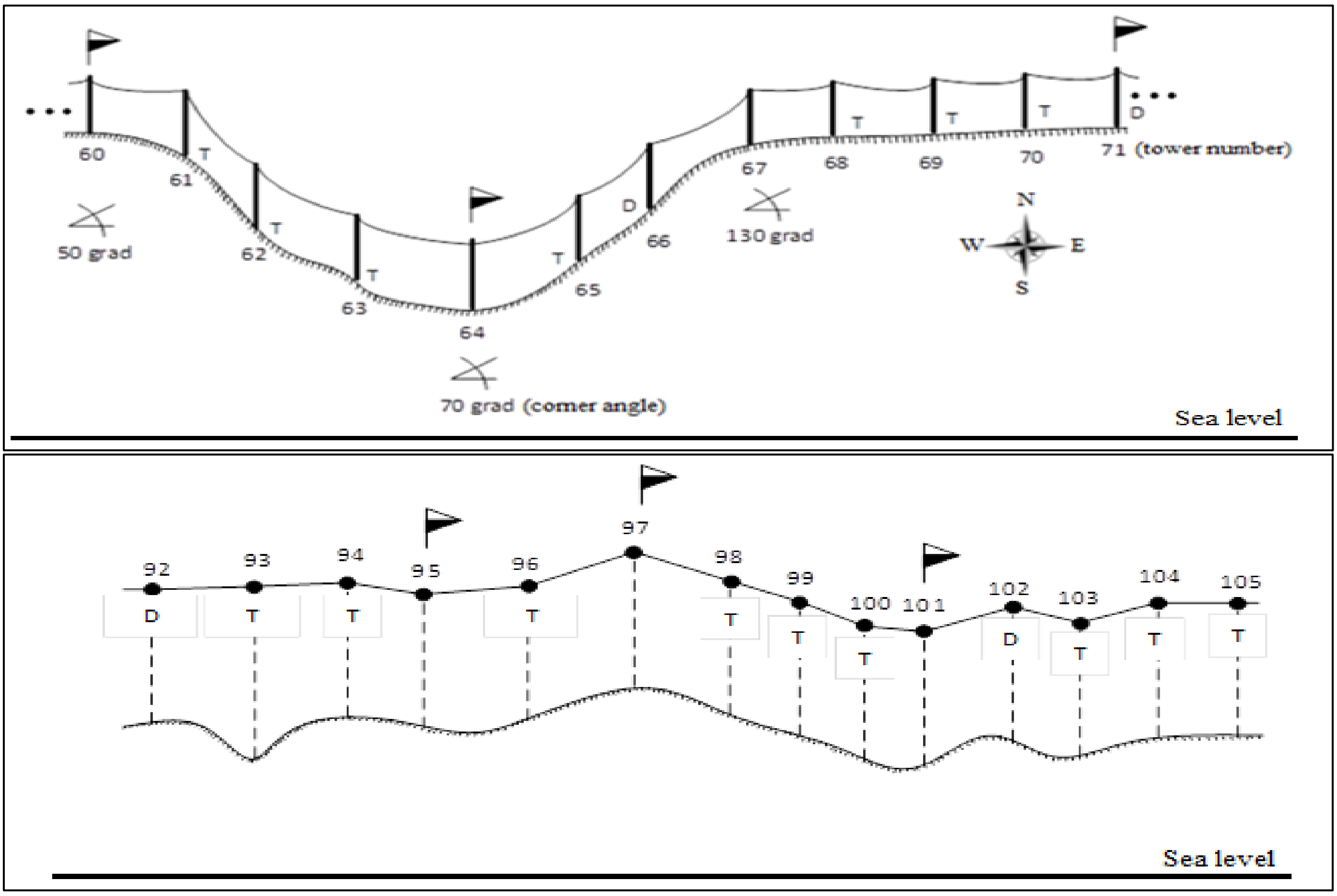

Fig 8: Land Sections for Circuit-1 and Circuit-2 in the Power Transmission System in Figure 7

ISSN No:-2456-2165 https://doi.org/10.38124/ijisrt/25mar1591

➢ *In Power Transmission Lines with Different Routes, the Following Properties Apply to Each Circuit:*

- The circuits are not parallel to each other.
- The directions of the circuits, the number of corner angles, and the lengths of the circuits are not the same.
- The operating voltage of the circuits is the same.
- The impedance (Ω/km) and admittance (S/km) of the circuits are the same.
- There is no mutual magnetic effect between the circuits.

Since the routes of the circuits are not in the same position relative to sea level, each circuit is under the influence of different meteorological parameters. For example, the air temperature decreases as the altitude above sea level increases. Table 3 shows the values that the temperature of 15 °C at sea level (H→0) will take as it increases above sea level.

Table 3: Standard Atmosphere Values [ISO 2533]

H (m)	T (°C)
0	15
500	11.8
1000	8.5
1500	5.3
2000	2.0
2500	–1.3
3000	–4.5

One of the empirical relations between altitude H (m) above sea level, air temperature t (ºC) and air pressure p (mmHg) is:

$$H=18464\times(1 + 0.0037\times t)\times(\ell og760 - \ell og\ p) \qquad (13)$$

Similarly, the amount of ultraviolet radiation that can reach the ground increases in direct proportion to the increase in altitude from sea level. Since the effect of absorbing parameters decreases as altitude increases, it is an inevitable result that the amount of radiation reaching the ground increases. Studies have determined that every 1000 meters of altitude causes an average increase of approximately 10% in ultraviolet radiation. On the other hand, "the amount of cloudiness (coverage rate)" is a very important definition in terms of expressing vertical visibility. It is the expression of how much of the sky, which is assumed to be divided into eight equal parts, is covered by clouds. Cloudiness plays a role in reducing insolation, prevents sunlight from reaching the earth and causes the temperature to drop. The Southern Hemisphere, where oceans cover a large area, is more cloudy than the Northern Hemisphere.

Table 4: Cloudiness Rates

Cloudiness	Ratio
Clear	0
Slight	1/8…2/8
Scattered	3/8…4/8
Partly	5/8…7/8

There is also a mathematical relationship between the altitude of the route above sea level (H) and the average wind force (v). For example, the following relationship can be used for 0 < H < 4000 m [27]:

$$v = -1.04\times z^4 + 1.127\times z^3 + 2.836\times z^2 + 1.677\times z + 4.115 \quad \ldots(m/s) \qquad (14)$$

Where

$$z = \frac{H-1644}{1346} \qquad (15)$$

In addition, when the wind speed measured at 10 m above the ground (v10) is taken as reference, the following relations are used for the wind speed (v) at a height of H (m) above the ground:

$$\frac{v}{v_{10}} = \left(\frac{H}{275}\right)^{1/9.5} \times 1.42 \qquad (16)$$

$$\frac{v}{v_{10}} = \left(\frac{H}{10}\right)^{0.16} \qquad (17)$$

When each circuit of a multi-circuit power transmission line is divided into n segments, the "meteorological parameters" for the calculation of the current carrying capacity of the j^{th} segment are as follows:

S_j: j. Solar radiation intensity of the jth segment (W/m^2)
$T_{max,j}$: Maximum ambient temperature of the j^{th} segment (°C)
v_j: Wind speed of the j^{th} segment (m/s)
a_j: Solar radiation coefficient of the j^{th} segment

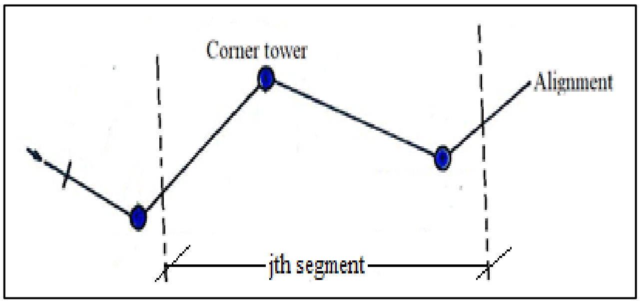

Fig 9: Bird's Eye View of a Power Transmission Line

The following factors can be taken into account in determining the number of segments (n) in each circuit:

- Is there a difference of more than ΔH = ± 100 meters in the altitude of the route above sea level?
- Is there a difference of more than ± 10° in the direction of the power transmission line?

The current carrying capacity ($I_{th,j}$)for the j^{th} segment in each circuit is calculated using equation (3). The minimum current value must be taken into account in order to satisfy the condition in equation (12):

$$I_{th} \rightarrow \min \{I_{th,j}\} \quad ; \quad j=1,2,\ldots,n \qquad (18)$$

In equation (3), if the average meteorological parameters of the segments in each period are used, S_{av}

ISSN No:-2456-2165 https://doi.org/10.38124/ijisrt/25mar1591

$T_{max,av}$ v_{av} a_{av}, the average ampacity is found. The following "weighted averages" are calculated, where $L = \sum_{j=1}^{n} L_j$:

$$S_{av} = \frac{\sum_{j=1}^{n} S_j \times L_j}{L} \tag{19}$$

$$T_{max,av} = \frac{\sum_{j=1}^{n} T_{max,j} \times L_j}{L} \tag{20}$$

$$v_{av} = \frac{\sum_{j=1}^{n} v_j \times L_j}{L} \tag{21}$$

$$a_{av} = \frac{\sum_{j=1}^{n} a_j \times L_j}{L} \tag{22}$$

If the "arithmetic mean" is used instead of the weighted mean for meteorological parameters:

$$x_{av} = \frac{\sum_{j=1}^{n} x_j}{n} \tag{23}$$

If the "geometric mean" is used for meteorological parameters:

$$x_{av} = \left(\prod_{j=1}^{n} x_j\right)^{1/n} \tag{24}$$

$$I_{th,av} = f(S_{av}, T_{max,av}, v_{av}, a_{av,}) \tag{25}$$

$$|\min\{I_{th,j}\} - I_{th,av}| = \varepsilon > 0 \tag{26}$$

The resistance of the unit length of the transmission line r (Ω/km) can be neglected since it is smaller than the reactance x (Ω/km). In this case, the impedance (reactance) of each circuit is approximately proportional to the length of the circuit. Let the current drawn from the load bus of the double-circuit power transmission line be I (Fig. 7). The currents that will pass through the first circuit of length L_1 and the second circuit of length L_2 must satisfy the condition in equation (12):

$$I_1 = I \times \frac{L_2}{L_1 + L_2} \leq I_{ACSR} \tag{27}$$

$$I_2 = I \times \frac{L_1}{L_1 + L_2} \leq I_{ACSR} \tag{28}$$

Similarly, in a power transmission system with three circuits and different routes, the condition in equation (12) must be satisfied for the currents that will pass through the 1st circuit of length L_1, the 2nd circuit of length L_2 and the 3rd circuit of length L_3.

$$I_1 = I \times \frac{\frac{L_2 \times L_3}{L_2 + L_3}}{L_1 + \frac{L_2 \times L_3}{L_2 + L_3}} \leq I_{ACSR} \tag{29}$$

$$I_2 = I \times \frac{\frac{L_1 \times L_3}{L_1 + L_3}}{L_2 + \frac{L_1 \times L_3}{L_1 + L_3}} \leq I_{ACSR} \tag{30}$$

$$I_3 = I - (I_1 + I_2) \leq I_{ACSR} \tag{31}$$

IV. NUMERICAL APPLICATION

In the three-circuit (k=3) power transmission system in Figure 10, the impedances (Ω/km) of all lines are identical, and their admittances (S/km) are neglected. All cage poles in the system are single-circuit. The voltages of the generator bars are equal. In terms of meteorology, 2 segments are determined for each transmission circuit in the system (j→1,2). T_J = 40 °C, the AC resistance of the 954 MCM cross-section ACSR conductor at 20 °C is 0.06 Ω/km (60 μΩ/m) and its diameter is 30.42 mm. For all circuits, e = 0.5 and a = 0.6 are assumed. The meteorological parameters vector (column matrix) defined for the jth segment in the kth circuit contains the parameters $[X_j]k \rightarrow S_j$ (W/m2), $T_{max,j}$ (°C), v_j (m/s):

$$[X_j]_k = [S_j\,(W/m^2),\ T_{max,j}\,(°C),\ v_j\,(m/s)]_k^T \quad ; \quad j \rightarrow 1,2 \quad ; k \rightarrow 1,2,3 \tag{32}$$

Where supercript T denotes transpose of the column matrix. Hypothetical $[X_j]$ vectors belonging to each segment in the 3-circuit power transmission line between bars 1-2 are given in Table 5. Meteorological parameters such as wind speed measured by anemometer, air temperature measured by thermometer, solar radiation intensity measured by pyranometer and pyrheliometer can be obtained from the meteorological center closest to the power transmission line or from the wind power plants and feasibility reports of wind power plants located in that region.

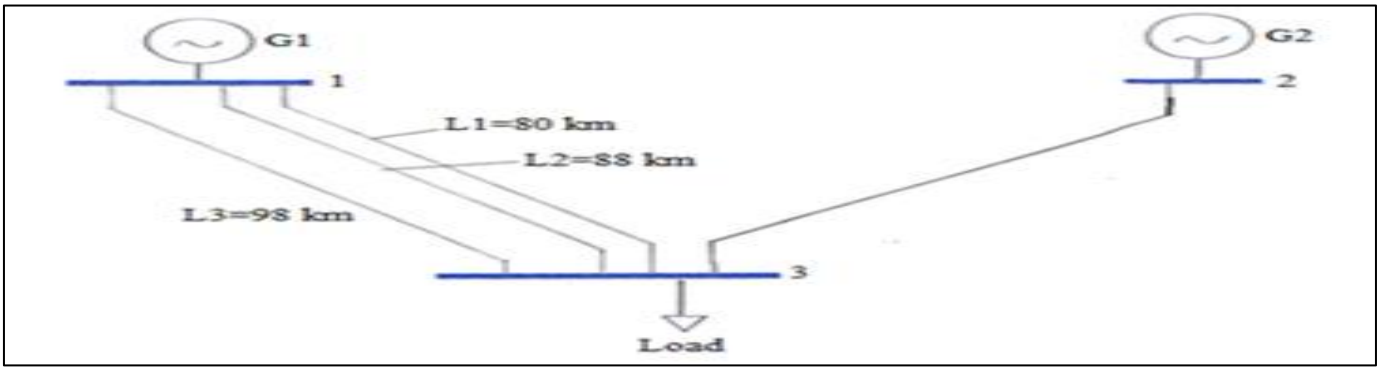

Fig 10: Considered Three-Circuit (k=3) Power Transmission System

ISSN No:-2456-2165 https://doi.org/10.38124/ijisrt/25mar1591

Table 5: Hypothetical [Xj] Vectors of L1, L2, L3 Circuits in the Sample System

Circuit	Segment 1	Segment 2
L1	$L_{j\to 1}$=20 km ; $[X_1]_1$=[900, 40, 1.1]^T	$L_{j\to 2}$=60 km ; $[X_2]_1$=[1000, 45, 0.9]^T
L2	$L_{j\to 1}$=30 km ; $[X_1]_2$=[950, 45, 0.91]^T	$L_{j\to 2}$=58 km ; $[X_2]_2$=[900, 40, 1.2]^T
L3	$L_{j\to 1}$=20 km ; $[X_1]_3$=[1100, 50, 0.8]^T	$L_{j\to 2}$=78 km ; $[X_2]_3$=[1000, 45, 1.0]^T

Table 6: Calculated Current Carrying Capacities of L_1, L_2, L_3 Circuits

Circuit	I_{th} (A)	I_{th} (A)[2]	I_{th} (A)[3]	I_{th} (A)[4]	I_{th} (A)[5]
L1	999.1 / 939.8[1]	955.2	970.2	969.2	966.0
L2	946.1[1] / 1018.2	993.2	984.1	982.0	985.4
L3	899.4[1] / 962.7	950.3	932.3	930.0	935.8

[1]Minimum value of segment currents along the line, min{$I_{th,jj}$}
[2]According to the weighted average of meteorological parameters along the line
[3]According to the arithmetic average of meteorological parameters along the line
[4]According to the geometric mean of meteorological parameters along the line
[5]Arithmetic average of the flows in the first four columns

V. CONCLUSION

The thermal current carrying capacities of multi-circuit power transmission lines with different routes are not equal. However, when a multi-circuit power transmission line is located on the same pole, the current carrying capacity of all circuits is equal. When each circuit is divided into segments and examined according to the altitude of the route above sea level and the condition of the land, different current carrying capacities can be calculated for each segment. The factor that determines the number of segments along a circuit is the absolute differences between the meteorological parameters of the segments.

The current carrying capacity can be calculated according to the weighted average or arithmetic average or geometric average of the meteorological parameters for each circuit.

When the continuous current carrying capacities calculated with the help of the data in Fig. 10 and Table 5 are examined, it is appropriate to consider the minimum value currents in the project for each circuit, considering the demand increase in the coming years (939.8 A, 946.1 A, 899.4 A for L1, L2, L3, respectively). The load current to be drawn from busbar 3 must meet the following condition in thermal terms: $I_{load} \le (I_{th})_{L1} + (I_{th})_{L2} + (I_{th})_{L3} + (I_{th})_{2\text{-}3}$. The distribution of the load current to the circuits is calculated using equations (29) and (30). Therefore, $I_{L1} \le (I_{th})_{L1}$, $I_{L2} \le (I_{th})_{L2}$, $I_{L3} \le (I_{th})_{L3}$.

When the demand power increases over time, the current carrying capacity of the existing conductors may not be sufficient; on the same poles, these conductors must be removed and replaced with conductors with higher current carrying capacity. Other ways to increase the current carrying capacity are to increase the number of bundles of the line (for example, converting a 2-bundle to a 3-bundle) or to use special conductors instead of ACSR.

REFERENCES

[1]. IEEE Standard 738 (2023)-Standard for Calculating the Current-Temperature Relationship of Bare Overhead Conductors.
[2]. IEC 61597 (1995)-Technical Report Type 3-Overhead electrical conductors: Calculation methods for stranded bare conductors.
[3]. CIGRÈ Brochure (2006)-Guide for Selection of Weather Parameters for Bare Overhead Conductor Rating, Technical Brochure 299.
[4]. CIGRÈ (2014)-Guide for Thermal Rating Calculation of Overhead Lines, Technical Brochure 601.
[5]. ESAA (The Electricity Supply Association of Australia) (1988)-Current Rating of Bare Overhead Line Conductors, D(lb) 5.
[6]. Schmidt, N.P., Comparison between IEEE and CIGRE Ampacity Standards", IEEE Transactions on Power Delivery, 14, 1555-1562, 1990.
[7]. Staszewski, L. and Rebizant, W. "The differences between IEEE and CIGRE heat balance concepts for line ampacity considerations", Modern Electric Powerr Systems (MEPS), Proceedings of the International Symposium, 2010, 1-4.
[8]. Bangay, J., Coleman, M., Batten, R., "Comparison of IEEE and CIGRE methods for predicting thermal behaviour of power lines and their relevance to distribution networks", 2015 IEEE Eindhoven Power Tech, 1-5.
[9]. Arroyo, A., Castro, P., Martinez, R., Manana, M., Madrazo, A., Lucuna, R., Gonzalez, A., "A comprarison between IEEE and CIGRE thermal behaviour standards and measured temperature on a 132 kV overhead power line", Energies, 8, 13660-13671, 2015.
[10]. Zenczak, M., "Approximate Relationships for calculation of current-carrying capacity of overhead power transmission lines in different weather conditions", Proceedings of the Progress in Applied Electrical Engineering (PAEE), 25-30 June 2017, Poland.
[11]. Spes, M., Bena, L., Kosterec, M. Marton, M., "Determining the current capacity of transmission

ISSN No:-2456-2165 https://doi.org/10.38124/ijisrt/25mar1591

lines based on ambient conditions", Journal of Energy Technology (JET), 10, 61-69, 2017.

[12]. Pavlinic, A. and Komen, V., "Calculation and anaysis of the steady-state line ampacity weather sensitivity coefficients", Electric Power Systems Research, 181, 106181, 2020.

[13]. Ghadiyali, A.A., Zinzuvadia, M.J., Choski, P.G., Grewal, G.S., "Prediction of temperature of overhead conductors using CIGRE thermodynamic model and its validation", International Journal of Advance Engineering and Research Development, 5, 2367-2379, 2018.

[14]. Coffey, J., "High temperature overhead conductor considerations", Transmission and Substation Design and Operations Symposium, September 5-8 2018, USA.",

[15]. Power EKanalik, M., Margitova, A., Urbanski, J., Bena, L., "Temperature calculation of overhead power line conductors according to CIGRE Technical Brochure 207", 20th International Scientific Conference on Electrical Engineering (EPE), 15-17 May 2019, Czech Republic.

[16]. Abboud, A.W., Gentle, J.P., Parikh, K., Coffey, J., "Sensitivity Effects of High Temperature Overhead Conductors to Line Rating Variables", Idaho National Laboratory (INL)", INL/CON-19-56930-Revision-0, 2020.

[17]. Gentle, J., Myers, K.S., Baldwin, T., West, I., Hart, K., Savage, B., Ellis, M., Anderson, P., "Concurrent wind cooling in power transmission lines", 2012 Western Energy Policy Research Conference, 30-31 August 2012, USA.

[18]. Rahman, S.A. and Kopsidas, K., "Impact of simplified convection model in overhead lines thermal rating calculation methods", 2018 IEEE/PES Transmission and Distribution Conference and Exposition (T&D), 16-19 April 2018, USA.

[19]. Riba, J.R, Liu, Y., Eguilaz, M.M., "Analyzing thee role of emisivity in stranded conductors for overhead power lines", International Journal of Electrical Power and Energy Systems, 159, 11027, 2024.

[20]. Deb, A.K., "Powerline Ampacity System: Theory, Modeling and Application", CRC Press, 2000.

[21]. Gomez, F.A., de Maria, J.M.G., Puertas, D.G., Bairi, A., Arrabe, R.G., "Numerical study of the thermal behaviour of bare overhead conductors in electric power lines", Proceedings of the 10th WSEAS International Conference on Communications, Electrical-Computer Engineering, March 24-26 2011, Canary Islands, Spain.

[22]. Sterc, T., Grcic, B.F., Franc, B., Mesic, K., "Methods for estimation of OHL conductor temperature based on ANN and regression analysis", International Journal of Electrical Power and Energy Systems, 151, 109192, 2023.

[23]. Malska, W., "Analysis of current ampacity of the 110 kV overhead transmission line using a multiple regression model", Electric Power Systems Research, 236, 110939, 2024.

[24]. Farzaneh, M., Farokhi, S. and Chisholm, W.A., "Electrical Design of Overhead Power Transmission Lines", McGraw-Hill, 2012.

[25]. Gonen, T., "Electrical Power Transmission Engineering: Analysis and Design", 3rd Edition, CRC Press, 2014.

[26]. TNSP Operational Line Ratings, Australian Energy Regulator (AER), 2007.

[27]. Solano, J.C., Montano, T., Correa, J.M., Ordonez, A., Pesantez, M., "Correlation between the wind speed and the elevation to evaluate the wind potential on the Southern Ecuador", 6th International Conference on Advances on Clean Energy Research (ICACER), April 15-17 2021, Spain.